A Bond Wire Aging Monitoring Method for IGBT Modules Based on Back Propagation Neural Networks

Gengle LIANG, Xinglai GE, Huimin WANG, Zhiliang XU, Dong LUO, and Yi WANG

***Abstract*—A typical degradation mechanism of insulated gate bipolar transistor (IGBT) modules is the bond wire degradation (BWD), and thus the bond wire aging monitoring (AM) shows much attractiveness for IGBT modules. However, the performance degradation with junction temperature swings and load current dependence in many bond wire AM methods remains an obstacle. To address this, a bond wire AM method based on the back propagation neural networks (BPNN) is proposed in this paper, in which the on-state voltage drop (OVD) is used as the indicator of bond wire AM. In the proposed AM method, a multi-physical field coupling model of the IGBT module is established. Then, with the assistance of the model, the characterization behaviors of the OVD are thoroughly analyzed. According to the analysis, it is known that the junction temperature swings and load current dependence may obviously degrade the performance of the proposed AM method. Afterward, BPNN is adopted to deal with these issues. Finally, the performance of the proposed AM method is explored through extensive experimental tests.**

***Index Terms*—Back propagation neural networks (BPNN), bond wire aging monitoring (AM), insulated gate bipolar transistor (IGBT) modules, multi-physical field coupling model.**

I. Introduction

INCREASING demands for a new paradigm of energy conversion necessitate the reliable operation of high-efficiency and high-power density converters [1]–[5]. In particular, the power modules, e.g., insulated gate bipolar transistor (IGBT) modules, in power converters are crucial because they are used to implement the task of energy conversion and power control.

However, the IGBT modules are regarded as one of the major contributors to the reliability degradation of power converters due to their high failure rate. Among many failure types of the IGBT modules, the bond wire degradation (BWD) is particularly prominent [6]–[8]. In this sense, accurate bond wire aging monitoring (AM) is desirable for ensuing the reliability of power converters.

Generally, the bond wire AM methods are classified into two groups, i.e., the direct AM methods [9]–[11] and the indirect AM methods [12]–[27]. Regarding to the direct AM methods, they are typically carried out by using special equipment, e.g., the eddy current pulsed thermography [9], the scanning electron microscope [10], and the acoustic detector [11], to detect the BWD without opening the shell of power modules. In spite of this, the direct AM methods are not appropriate for real-time applications. Moreover, these methods usually suffer from high complexity and cost because of the use of additional detection equipment. The indirect AM method accomplishes the task of bond wire AM by monitoring the electrical parameters associated with the BWD without destroying the device, making it suitable for online applications.

According to the type of the used electrical parameters, the indirect AM methods are further divided into the static electrical parameter (SEP) methods and the dynamic electrical parameter (DEP) methods. The SEP methods use the electrical parameters that are not involved in the turn-on and the turn-off transient processes to implement the bond wire AM [12]–[19]. Among them, as detailed in [12], it had been experimentally investigated that the bond wire aging will lead to an apparent increase of the on-state voltage drop (OVD). However, this method is highly affected by junction temperature swings. To address this, a SEP method based on the on-state voltage at inflection point is proposed in [13], and a major contribution of this method is able to monitor the BWD and be irrespective of the junction temperature swings. Whereas, this bond wire AM method is implemented at the fixed load current, which, however, is inapplicable because the load current of the IGBT module will obviously vary in practice. Following that, [14] revealed that the short-circuit current shows a high sensitivity to the BWD, and more importantly, this indicator of the BWD is free from the effects of junction temperature swings. Unfortunately, the short-circuit current of the IGBT module is barely measurable when the power converters are operating.

Alternatively, considerable research efforts have been

Manuscript received June 7, 2023; revised August 26, 2023; accepted December 5, 2023. Date of publication March 30, 2024; date of current version December 19, 2023. This work was supported by Key Laboratory of Railway Industry of Maglev Technology (TJU) National Railway Administration of P.R.C under Grant 202203. *(Corresponding author: Xinglai Ge.)*

G. Liang, X. Ge, Z. Xu, D. Luo, and Y. Wang are with the School of Electrical Engineering, Southwest Jiaotong University, Chengdu 610031, China (e-mail: liang_geng_le@my.swjtu.edu.cn; xlge@swjtu.edu.cn; xzl@my.swjtu.edu.cn; 2694864497@qq.com; wangyi@swjtu.edu.cn).

H. Wang is with Key Laboratory of Railway Industry of Maglev Technology (TJU), National Railway Administration of P.R.C, Shanghai 201804, China (e-mail: 1152410117@qq.com).

Digital Object Identifier 10.24295/CPSSTPEA.2023.00048

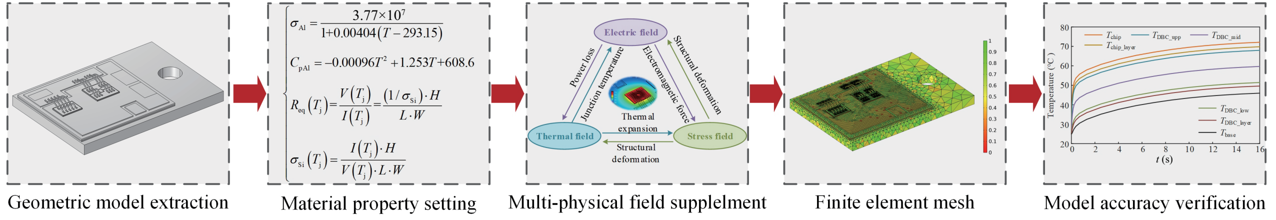

Fig. 1. Block diagram of the multi-physical field coupling model of the IGBT module.

developed towards utilizing the DEP methods to enhance the performance of bond wire AM [20]−[27]. Though the flourishing developments of the bond wire AM methods are observed in the considerable literature, most of these methods are troubled by the challenging issues like junction temperature swings and load current dependence.

Recently, a new paradigm in the research of reliability evaluation of power modules is to use the artificial intelligence (AI) techniques [28]−[35], in which the neural networks, the machine learning, and the digital twins are notable examples. In [29], the artificial neural networks were assisted in the thermal model for power modules to handle the troublesome problem of thermal cross-coupling effects. Additionally, a noninvasive condition monitoring method for power converters based on the digital twins is reported in [32], and the degradation trends of power modules can be effectively observed. Following that, [34] provided a physics-informed machine learning-based condition monitoring method for power converters, and respectable achievements of high accuracy and strong robustness are developed. Moreover, a deep learning method is adopted in [35] to conduct the maximum junction temperature estimation for multichip power modules.

In light of the above, a bond wire AM method for IGBT modules based on the back propagation neural networks (BPNN) is proposed in this paper, which takes OVD as a static electrical parameter and eliminates the influence of temperature swings and load current well. The rest of this paper is organized as follows. In Section II, the multi-physics field coupling model of IGBT module is provided, and the accuracy of the model is carefully verified. In Section III, based on theoretical analysis and the multi-physics field coupling model, the characterization behavior of OVD is analyzed comprehensively. It can be clearly seen that junction temperature swings and load current dependence will adversely affect the use of OVD for bond wire AM. Following that, BPNN is used to ensure the performance of bonded wire AM with junction temperature swings and load current dependence, as detailed in Section IV. Finally, extensive experimental tests are carried out to investigate the performance of the proposed AM method under different operating conditions. The main contributions are as follows：

- A bond wire aging monitoring method for IGBT is proposed, and the issues of junction temperature swing and load current dependence can be avoided effectively in this method.
- BPNN is introduced to solve the complex coupling relationship of junction temperature, load current, OVD and wire aging, compared with traditional methods, which improves the resolution and accuracy of detection.
- The proposed AM method has satisfactory performance for the monitoring of early bond wire aging.
- A multi-physics filed coupling model of IGBT is established, which allows for a comprehensive analysis of OVD behavior under different conditions.

Fig. 2. Open-shelled IGBT module of Infineon FF50R12RT4.

II. Multi-Physical Field Coupling Model of the IGBT Modules

The measured SEP is difficult to reveal the bond wire degradation directly because of the dependence of temperature the current. In this section, a multi-physical field coupling model of an IGBT module is established. The quantified coupling effects serve as a fundamental of analyzing the relationship between the measured SEP and the degradation.

Fig. 1 shows the block diagram of the multi-physical field coupling model of the IGBT module, in which there are five steps involved in the establishment of this model, i.e., the geometric model extraction, the material property setting, the supplement of the multi-physical field, the generation of the finite element mesh, and the verification of model accuracy.

As for the extraction of the geometric model, it is accomplished by obtaining the geometric parameters and determining the geometric position of each layer. In this paper, the IGBT module of Infineon FF50R12RT4 is used as a case study, and the open-shelled IGBT module is presented in Fig. 2. With this, some of geometric parameters are measurable, and several geometric parameters can be obtained from the data sheet of Infineon FF50R12RT4. Moreover, due to the irregular geometric structure of the upper copper layer, the geometric position of the upper copper layer is depicted in Fig. 3, in which the number is the dimension parameter and the unit is

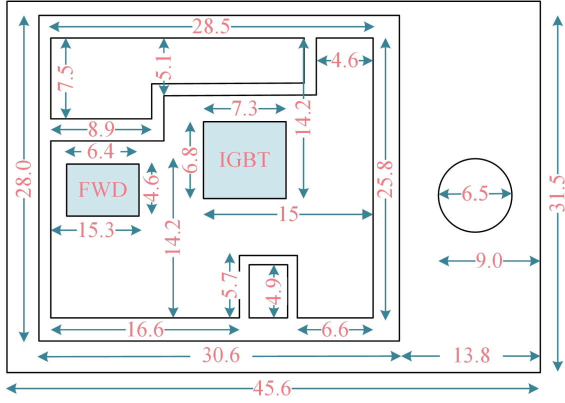

Fig. 3. Geometric position of the upper copper layer.

millimeter. Accordingly, the geometric model is obtained.

After extracting the geometric model, the material properties of the IGBT modules should be properly set. According to the data sheet of the IGBT module and the material property, the conductivity and the heat capacity at constant pressure of the bond wire (its material is aluminum) can be fitted as [36], [37]:

$$\begin{cases} \sigma_{\mathrm{Al}} = \dfrac{3.77\times10^{7}}{1+0.00404(T-293.15)} \\ C_{\mathrm{pAl}} = -0.00096T^{2}+1.253T+608.6 \end{cases} \tag{1}$$

with T being the Kelvin temperature. Additionally, the material of the IGBT chip is silicon, and its conductivity of the IGBT chip is affected by the junction temperature and the load current. Considering this, the equivalent resistance of the IGBT chip at the junction temperature is given by

$$R_{\mathrm{eq}} = \frac{V_{\mathrm{ce}}}{I_{\mathrm{c}}} = \frac{1}{\sigma_{\mathrm{Si}}}\frac{H}{LW} \tag{2}$$

in which R_{eq}, V_{ce}, I_{c}, H, L, W, and σ_{Si} are the equivalent resistance of the IGBT chip, the OVD that is affected by junction temperature, the current of the IGBT module, the thickness of the IGBT chip, the length of the IGBT chip, the width of the IGBT chip, and the conductivity of silicon, respectively. Subsequently,

$$\sigma_{\mathrm{Si}} = \frac{I_{\mathrm{c}}H}{V_{\mathrm{ce}}LW} \tag{3}$$

According to the output I-V characteristic curve of the data manual and conductivity expression [38], and combined with MATLAB curve fitting toolbox, the conductivity of silicon can be obtained that

$$\sigma_{\mathrm{Si}}(T_{\mathrm{j}}, I_{\mathrm{c}}) = \frac{1.126\times10^{7} I_{\mathrm{c}}}{2.826\times10^{6}+4.02\times10^{4} I_{\mathrm{c}}+6161T_{\mathrm{j}}+321.4I_{\mathrm{c}}T_{\mathrm{j}}} \tag{4}$$

Similarly, the heat capacity of silicon at constant pressure is calculated as [39]

$$C_{\mathrm{pSi}} = 5.27\times10^{-6}T^{3}-8.43\times10^{-3}T^{2}+4.77T-108.1 \tag{5}$$

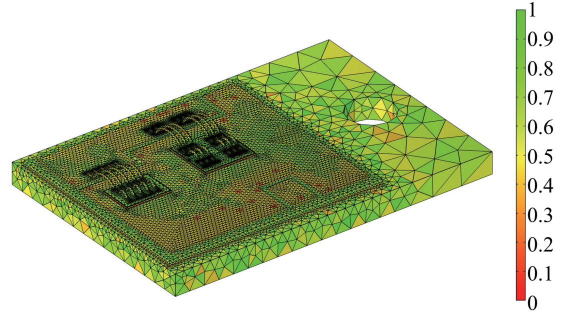

Fig. 4. Finite element mesh of the IGBT module.

Moreover, the material of both the baseplate layer and the direct bond copper layer is copper, and the conductivity and the heat capacity of copper at constant pressure are described as:

$$\begin{cases} \sigma_{\mathrm{Cu}} = \dfrac{5.95\times10^{7}}{1+0.00404(T-293.15)} \\ C_{\mathrm{pCu}} = -2.25\times10^{-4}T^{2}+0.2927T+317.7 \end{cases} \tag{6}$$

Then, the multi-physical field is supplemented to analyze the coupling effects, which includes the setting of the related constraints and the introduction of the multi-physical coupling. Additionally, a combination of the thermal field and the stress field is developed, and eventually the electric-thermal-stress coupling of the IGBT module is made. To ensure model accuracy and computational efficiency, the user-defined mesh method is used. More specifically, the tetrahedron mesh method and the triangular mesh are adopted for the bond wire and the IGBT chip, respectively. Notably, the free mesh method and the subdivision mesh method are applied for the baseplate and the other layers, and the finite element mesh of the IGBT module is shown in Fig. 4.

As mentioned previously, the model is of importance for the characterization behaviors of the IGBT modules. Due to this, the model accuracy is further evaluated. The I-V characteristic curves of the IGBT module provided by the multi-physical coupling model are compared to those of the data sheet with different junction temperature, which is shown in Fig. 5. Observations in Fig. 6 indicate that the characteristic curves of the multi-physical coupling model under different junction temperature agree with those of the data sheet well. Moreover, another comparison between the multi-physical coupling model and the data sheet in terms of thermal transient curve, and the results are shown in Fig. 6. As shown, a satisfactory agreement between the thermal transient curve of the proposed model and that of the data sheet is made, which justifies the accuracy of the multi-physical coupling model.

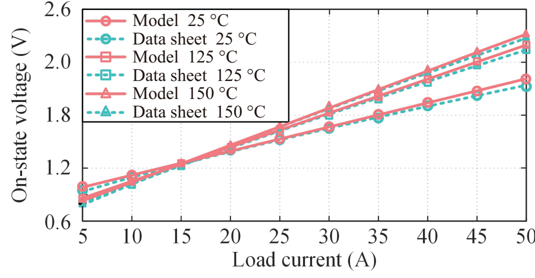

Fig. 5. Performance comparison between the multi-physical coupling model and the data sheet in terms of I-V characteristic curves.

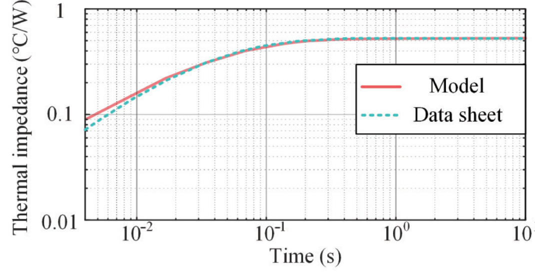

Fig. 6. Performance comparison between the multi-physical coupling model and the data sheet in terms of thermal transient curves.

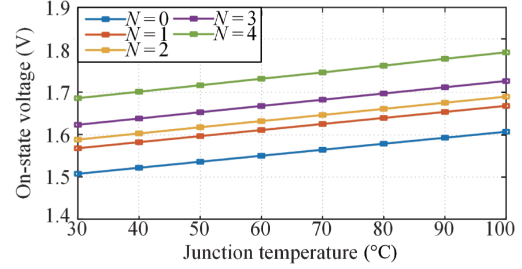

Fig. 7. Characterization behavior of the OVD with different numbers of lift-off bond wires.

III. Characterization Behavior Analysis of the On-State Voltage Drop With the Effects of Bond Wire Degradation

In the proposed AM method, the OVD is used as the indicator of the BWD. Considering this, in this section, the characterization behaviors of the OVD with different operation conditions are analyzed in detailed based on the multi-physical field coupling model.

A. Characterization Behavior Analysis of the On-State Voltage Drop With the Effects of Bond Wire Lift-Off

The characterization behaviors of the OVD with different numbers of lift-off bond wires are first analyzed. The OVD of the IGBT module can be expressed as [16]:

$$V_{ce}=R_{ce}I_c+V_{ce0} \tag{7}$$

in which R_{ce} and V_{ce0} are the on-state resistance and the intersection point of the horizontal axis of the I-V curve, respectively. And,

$$R_{ce}=R_{chip}+R_{bond}+R_{copper}+R_{term} \tag{8}$$

in which R_{chip}, R_{bond}, R_{copper}, and R_{term} are the equivalent resistance of the IGBT chip, the equivalent resistance of the bond wire, the equivalent resistance of the copper layer, and the equivalent resistance of the terminal, respectively. When the bond wire lift-off occurs, the increase of the on-state resistance can be observed. Consequently, the OVD is increased with the effects of bond wire lift-off, and shows a good sensitivity to the BWD, which can be seen in Fig. 7. With this characteristic, the OVD is selected as the indictor of the BWD.

B. Characterization Behavior Analysis of the On-State Voltage Drop With Load Current Variations

Additionally, the effects of junction temperature swings on the characterization behaviors of the OVD are explored. The internal structure of the IGBT is shown in Fig. 8. The IGBT model in on-state state can be simplified as a P-i-N rectifier in series with a MOSFET operating in the triode region.

The on-state voltage when the MOSFET section operates in the triode region can be expressed as [40]:

$$V_{MOS}=\frac{ZL_{CH}J_{C}}{\mu_{ni}C_{OX}\left(V_{G}-V_{TH}\right)} \tag{9}$$

where Z is the cell pitch, L_{CH} is the channel length, J_C is the collector current density, μ_{ni} is the inversion layer electron mobility, C_{OX} is the specific capacitance of the gate oxide, V_G is the gate bias voltage, and V_{TH} is the threshold voltage.

Then, the on-state voltage of the P-i-N rectifier can be expressed as:

$$V_{PiN}=\frac{2kT}{q}\ln\left[\frac{J_{C}d}{2qD_{a}n_{i}F\left(d/2L_{a}\right)}\right] \tag{10}$$

Function $F(d/2L_a)$ is given by:

$$F\left(\frac{d}{L_{a}}\right)=\frac{\left(d/L_{a}\right)\tanh\left(d/L_{a}\right)}{\sqrt{1-0.25\tanh^{4}\left(d/L_{a}\right)}}e^{-\frac{qV_{M}}{2kT}} \tag{11}$$

where k is the Boltzmann constant, T is the temperature, q is the elementary charge, d is a half of drift region thickness, D_a is the bipolar diffusion coefficient, n_i is the intrinsic carrier concentration, L_a is the bipolar diffusion length, and V_M is the voltage drop on the drift region.

Thus, the on-state voltage of IGBT can be expressed as:

$$\begin{aligned}V_{IGBT}&=V_{PiN}+V_{MOS}\\&=\frac{2kT}{q}\left(\ln(J_{C}d)-\ln\left(\frac{2qD_{a}n_{i}\left(d/L_{a}\right)\tanh\left(d/L_{a}\right)}{\sqrt{1-0.25\tanh^{4}\left(d/L_{a}\right)}}\right)\right)\\&\quad+V_{M}+\frac{ZL_{CH}J_{C}}{\mu_{ni}C_{OX}\left(V_{G}-V_{TH}\right)}\end{aligned} \tag{12}$$

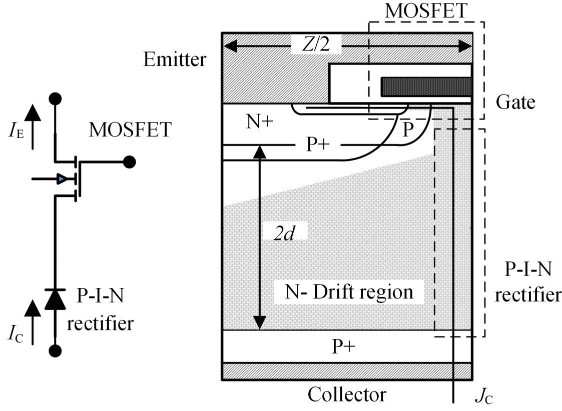

Fig. 8. One-dimensional structure of IGBT simple model.

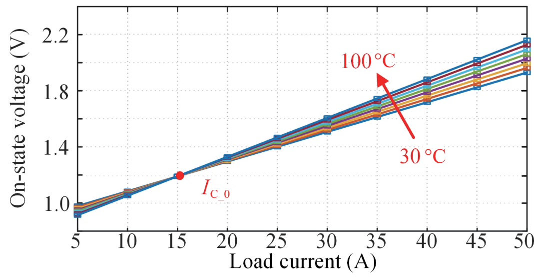

Fig. 9. Characterization behavior of the OVD with different load currents and junction temperature.

In (11), the first term predominates when J_C is low, i.e., the IGBT conducts with small current. When the collector current density is large, i.e., when the IGBT conducts with large current, the third term dominates. In this case, the collector current of the IGBT increases linearly with the increase of the on-state voltage drop. Generally, in the linear region OVD is treated as a parameter for AM.

Referring to (12), the load current is involved in the OVD. Due to this, the characterization behaviors of the OVD are further investigated with load current variations based on the coupled multi-physical field model. In this case, the junction temperature is increasing, and the variations of the load current from 5 A to 50 A are applied. The simulation results are shown in Fig. 9, clearly, different load currents result in different characterization behaviors of the OVD. That means, the load current will significantly affect the performance of the OVD.

C. Characterization Behavior Analysis of the On-State Voltage Drop With Junction Temperature Swings

To emphasize the effects of temperature on OVD, (12) can be expressed linearly as [41]:

$$V_{\mathrm{IGBT}} = \left(\frac{\mathrm{d}V_{\mathrm{IGBT}}}{\mathrm{d}T}\right)_{I_c} T + V_{\mathrm{IGBT_0}} \tag{13}$$

The coefficient $\left(\frac{\mathrm{d}V_{\mathrm{IGBT}}}{\mathrm{d}T}\right)_{I_c}$ is correlated with I_C. When I_C is equal to current threshold I_{C_0}, OVD has no temperature dependent; when $I_C>I_{C_0}$, coefficient $\left(\frac{\mathrm{d}V_{\mathrm{IGBT}}}{\mathrm{d}T}\right)_{I_c}>0$, OVD is positively correlated with temperature; conversely, coefficient $\left(\frac{\mathrm{d}V_{\mathrm{IGBT}}}{\mathrm{d}T}\right)_{I_c}<0$, OVD is negatively correlated with temperature, as shown in Fig. 9. That is, the OVD is challenged by the issue of junction temperature swings, which may make the proposed AM method suffer from obvious performance degradation with different junction temperature.

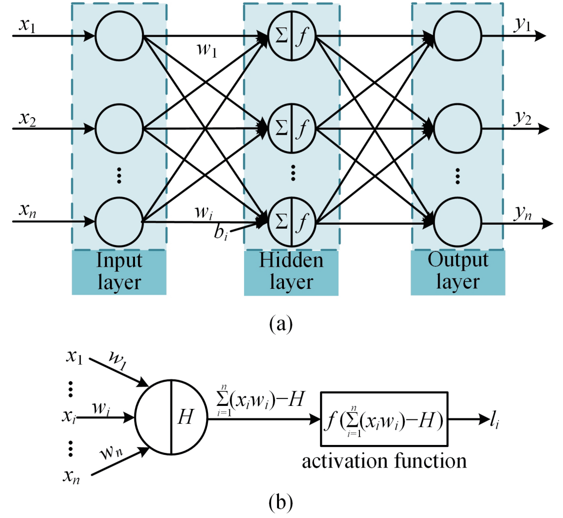

Fig. 10. Block diagram of the typical BPNN: (a) the structure of the BPNN and (b) the structure of the hidden layer.

From the above analysis, it is known that the OVD is accompanied by the challenges of junction temperature swings and load current dependence. A viable solution to these troublesome problems is provided by using the BPNN, which is elaborated in the next section.

IV. Implementations of the Proposed Bond Wire Aging Monitoring Method Based on the BPNN

The OVD is criticized for performance degradation with junction temperature swings and load current dependence. To address this, a bond wire AM method based on the BPNN is proposed, and the implementations of the proposed AM method are provided in this section.

A. Basics of Back Propagation Neural Networks

As one of widely-used neural networks techniques, features like strong nonlinear mapping ability and flexible network structure make the BPNN attract much popularity. The BPNN that is based on the gradient descent method, is a multi-layer feedforward network trained by using the error back propagation method [42].

Fig. 10 shows the block diagram of the BPNN, which includes the input layer, the hidden layer, and the output layer. $x_1, x_2, \ldots, x_n$ and $y_1, y_2, \ldots, y_n$ are the n-dimensional input and output of every sample in the BPNN. And, w_i and b_i (i = 1, 2,

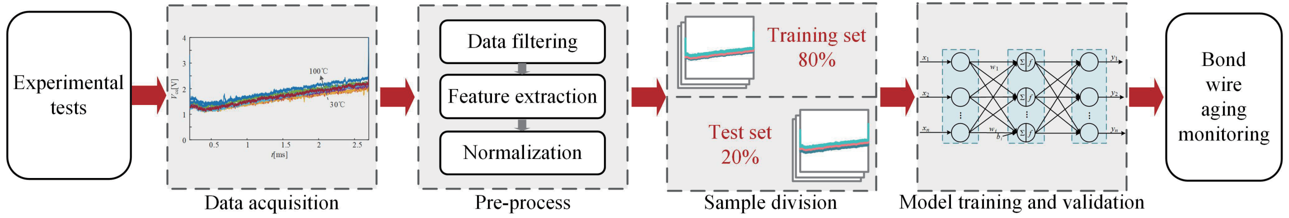

Fig. 11. Block diagram of the proposed bond wire aging monitoring (AM) method based on the back propagation neural networks (BPNN).

…, n) are the connection weight between the previous layer of neurons and the next layer of neurons, and the offset that is used for proper data fitting, respectively. The hidden layer is of importance for the BPNN, which mainly includes the sum operation and the activation function (see Fig. 10(b)). In the hidden layer, the use of the activation function is able to enhance the non-linearity, and hence, the performance improvement of the BPNN is made. There are two processes in the BPNN, i.e., the forward propagation and the back propagation. More specifically, in the forward propagation, the inputs undergo the nonlinear transformation through the hidden layer to generate the outputs. When checking the large errors between the reference output and the actual output, the back propagation is accordingly implemented. That is, the errors are transmitted through the hidden layer to the input layer. Then, the connection weight and the offset are adjusted to make the errors decrease along the gradient direction. In this way, the target of error minimization is eventually achieved.

B. Practical Implementation of the Proposed Bond Wire AM Method

Fig. 11 illustrates the block diagram of the proposed AM method based on the BPNN, in which five steps are involved in the implementations of the proposed AM method, i.e., the data acquisition, the pre-process, the sample division, the model training and validation, and the bond wire AM.

At first, extensive experimental tests are carried out to obtain OVD data of IGBT module at different load currents, different junction temperatures and different bond wire aging degrees. The test conditions are given in Section V. Then, the data of the OVD are pre-processed to guarantee the features of the OVD. That is, the collected data of the OVD are filtered to mitigate the effects of noise. And, the features of the OVD are extracted from these filtered data. Meanwhile, the extracted features of the OVD are normalized to remove the dimensional effects and eliminate the singular sample. With this, both the training time and the model convergence of the BPNN are maintained. In the proposed AM method, the maximum-minimum normalization method is used to make the extracted features normalize within the range of [0,1], which is described as

$$\overline{x}_i = \frac{x_i - x_{\min}}{x_{\max} - x_{\min}} \tag{14}$$

in which $\overline{x}_i$, x_i, $x_{\min}$, and $x_{\max}$ are the normalized feature of the training sample, the i-dimensional feature of the training sample, the minimum value and the maximum value of the training sample, respectively.

Afterward, the processed features of the OVD are further divided into the training set and the test set with an appropriate ratio of the number of the training set to the test set. In the proposed AM method, 80% of the samples of the OVD are used for the training set while the test set includes 20% of the samples of the OVD. A further process of random shuffling the training samples is implemented to improve the convergence speed. By doing so, the effects of overfitting are avoided and the generalization ability of the BPNN is improved. Moreover, as a supervised learning method, the training sample in the BPNN should be labeled, and in the proposed AM method, the number of lift-off bond wire is used as the label of the BPNN.

The fourth step of the proposed AM method is the model training and validation, which is crucial for the proposed AM method. The architecture of the BPNN and the initialization of the BPNN are first performed. Notably, the number of the input layer neurons is the dimension of sample feature while the number of the hidden layer neurons is determined according to the test results of the BPNN. As discussed previously, the activation function shows high importance in the BPNN and different types of activation functions are employed in the BPNN, which are given in (15)-(17). That is, the sigmod function and the tansig function are adopted in the input layer and the hidden layer, respectively. While, the output layer uses the purelin function as the activation function.

$$\mathrm{sig\,mod}(x) = \frac{1}{1+\mathrm{e}^{-x}} \tag{15}$$

$$\tan \mathrm{sig}(x) = \frac{1-\mathrm{e}^{-2x}}{1+\mathrm{e}^{-2x}} \tag{16}$$

$$\mathrm{purelin}(x) = x \tag{17}$$

As for the initialization of the BPNN, the training times and the training target are set to 300 and 0.01, respectively. Specifically, the training target means the errors between the reference and the output of the BPNN during the training processes of every sample. Moreover, the learning rate of the BPNN should be carefully considered. This is because that a small learning rate makes the BPNN get stuck at local optimum, and the BPNN model suffers from a slow convergence. By contrast, the BPNN with a large learning rate may swings at the minimum value, and even cause the divergence of the BPNN. In the proposed AM method, the learning rate is set to 0.02. Then, in the training set, the Levenberg-Marquardt

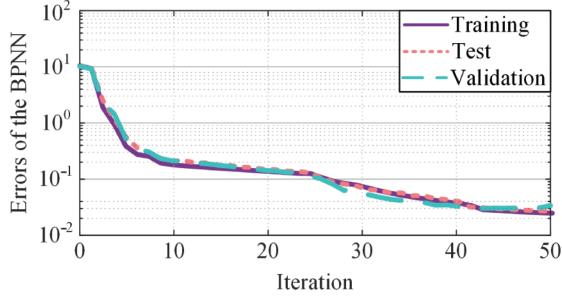

Fig. 12. Training processes of the BPNN.

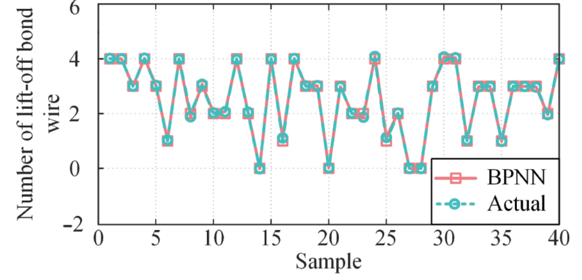

Fig. 13. Performance the proposed AM method with the well-trained BPNN.

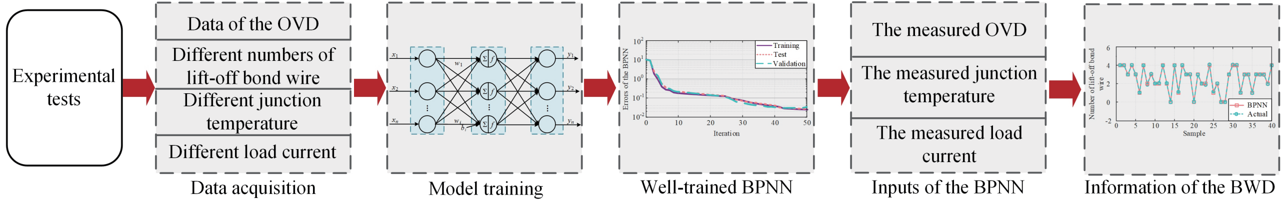

Fig. 14. Solution of the proposed AM method to junction temperature swings and load current dependence.

method is used to implement the task of minimizing the errors between the reference and the output of the BPNN, aiming at a satisfactory training performance of the BPNN. In this method, the Gaussian-Newton algorithm is employed to iteratively optimize the parameters of the BPNN. Meanwhile, an attenuation coefficient is introduced in the BPNN to perform a quick convergence and the attenuation coefficient will be adjusted according to the errors of the BPNN. When the errors meet the requirements, the model of the BPNN is identified as well-trained. Eventually, with the assistance of the well-trained model, accurate AM of bond wire is achieved. The training process of the BPNN is shown in Fig. 12. Seen from Fig. 12, after 40 iterations, the errors of the training set and the test set are obviously decreased, and the errors of the BPNN approach the training target (i.e., 0.01), which demonstrates that an acceptable training performance of the BPNN is achieved. Then, the performance of the proposed AM method with the well-trained BPNN is examined, which is presented in Fig. 13. Observations in Fig. 13 suggest that with the assistance of the well-trained model, the proposed AM method exhibits a satisfactory performance in terms of bond wire AM.

C. Performance of the Proposed AM Method With Junction Temperature Swings and Load Current Variations

As mentioned previously, the OVD is obviously affected by junction temperature swings and load current dependence. To address this, in the proposed AM method, solution to junction temperature swings and load current variations is provided, which is shown in Fig. 14. That is, the data of the OVD under different numbers of lift-off bond wires, different load currents and different junction temperature are collected (see Fig. 15). Then, with these collected OVD, the BPNN for bond wire AM is effectively trained. Subsequently, the measured OVD, the measured junction temperature and the measured load current

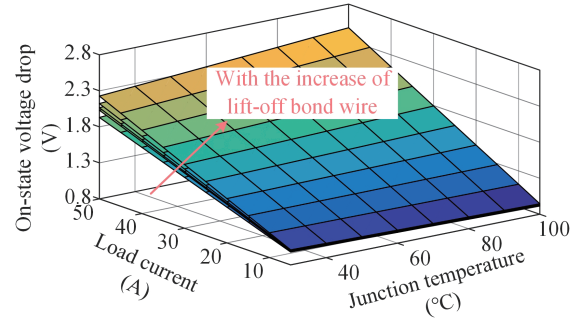

Fig. 15. Performance of the OVD with different numbers of lift-off bond wires, different load currents and different junction temperature.

are used as the inputs of the well-trained BPNN, and the information of the BWD is obtained. By doing so, the task of bond wire AM is accomplished and the effects of junction temperature swings and load current dependence are avoided.

D. Performance of the Proposed AM Method for Early Bond Wire Aging

In practice, in addition to the complete lift-off, there are also early bond wire aging manifestations such as cracks. The early aging is difficult to monitor. In order to explore the performance of proposed AM method for cracks, simulation for bond wire cracks is added based on multi-physical field coupling model.

As the cracks affect the contact area of the bond wire solder point, the contact resistance of the solder point increases. A method based on adjusting the contact resistance of the bond wire weld joints is used to simulate the diffusion process of cracks, and a schematic diagram of the contact resistance of the solder joints is given in Fig. 16. A random setting of 18 groups with different cracking degrees and current conditions are used as samples for analysis, as shown in Table I.

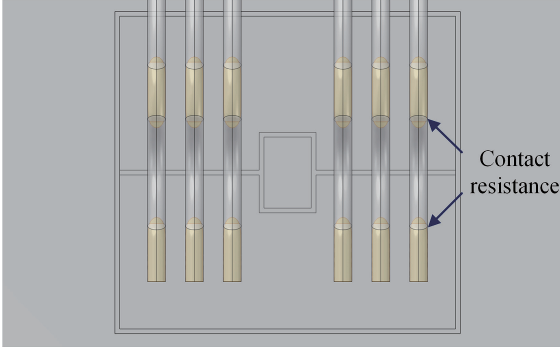

Fig. 16. Contact resistance of bond wire solder joints (yellow marking).

TABLE I
BOND WIRE EARLY AGING TEST SAMPLE

Sample	R_{bonding}	Current	Sample	R_{bonding}	Current
1	0.002 Ω	35 A	10	0.002 Ω	42 A
2	0.003 Ω	30 A	11	0.004 Ω	6 A
3	0.005 Ω	20 A	12	0.006 Ω	17 A
4	0.005 Ω	50 A	13	0.007 Ω	9 A
5	0.006 Ω	25 A	14	0.008 Ω	23 A
6	0.007 Ω	45 A	15	0.009 Ω	34 A
7	0.008 Ω	15 A	16	0.010 Ω	55 A
8	0.009 Ω	10 A	17	0.010 Ω	34 A
9	0.002 Ω	47 A	18	0.012 Ω	18 A

In the previous simulation, the contact resistance is set to 0.002 Ω for the healthy case of the bond wire. It is tested that when bond wire contact resistance is set to 0.0125 Ω, it is equivalent to the case of only one lift-off bond wire. Then, based on function fitting, the relationship between the bond wire contact resistance and the number of lift-off numbers N ($N < 1$) can be given by

$$N = 0.9749e^{0.1541\frac{R_{\text{bonding}}-0.002}{0.0125-0.002}} + 0.0251e^{0.9681\frac{R_{\text{bonding}}-0.002}{0.0125-0.002}} - 1 \quad (18)$$

Eighteen samples of different working conditions are used as inputs to the well-trained BPNN bond wire aging monitoring model. Finally, the cracks simulation samples output results and the results obtained according to (18) are shown in Fig. 17. It can be seen that the error is in a small range, which indicates that the proposed AM method performs well for monitoring early aging such as bond wire cracks.

V. EXPERIMENTAL RESULTS

To illustrate the effectiveness of the proposed AM method, the experimental tests based on the test bench in Fig. 18 are carried out, and the test cases are listed in Table II. Seen from Fig. 18, the experimental test bench consists of an infrared thermometer (Optris LT-CF2-CB3), the DC-link capacitors, the inductance, the heating plate, the driver board, the signal generator, the voltage sensor, the current sensor, the DC power supply, the oscilloscope, the host computer, and the tested

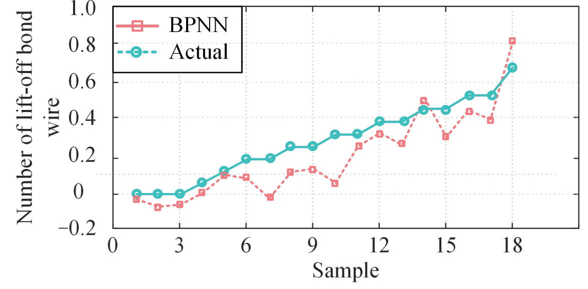

Fig. 17. Bond wire monitoring performance of the proposed AM method by using the cracks simulation samples.

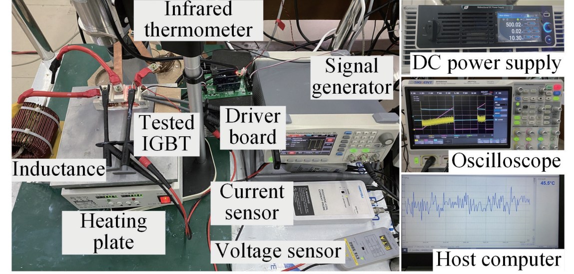

Fig. 18. Photo of the experimental set-up.

TABLE II
TEST CASES IN THE EXPERIMENTAL TESTS

Test case	Junction	Load current	Number of lift-off
Case 1	88 °C	5 A:5 A:40 A	0
Case 2	95 °C	5 A:5 A:40 A	0
Case 3	85 °C	5 A:5 A:40 A	1
Case 4	95 °C	5 A:5 A:40 A	1
Case 5	65.5 °C	5 A:5 A:40 A	2
Case 6	75 °C	5 A:5 A:40 A	2
Case 7	78.1 °C	5 A:5 A:40 A	3
Case 8	101.9 °C	5 A:5 A:40 A	4

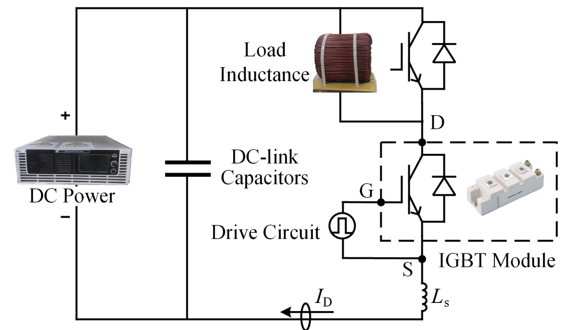

Fig. 19. Experimental circuit topology for double pulse test.

IGBT module (Infineon FF50R12RT4). Notably, in the experimental tests, the load current is varied from 5 A to 40 A with the interval of 5 A. It is difficult to quantify the aging degrees of the bond wire in the experiment, thus, the bond wire aging is simulated by stripping the bond wire, the number of lift-off bond wire is varied from 0 to 4, and the junction temperature is

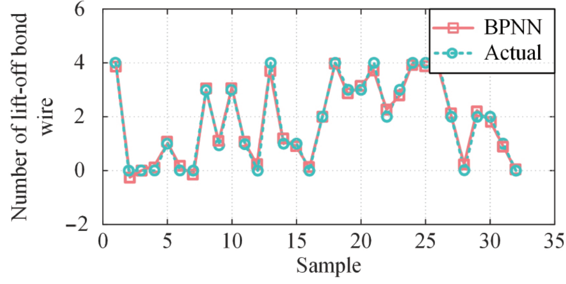

Fig. 20. Bond wire monitoring performance of the proposed AM method by using the experimental tests.

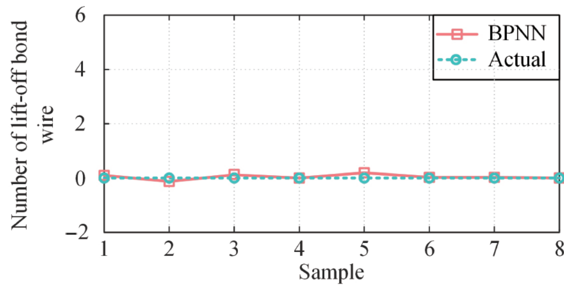

Fig. 21. Performance of the proposed AM method under case 1.

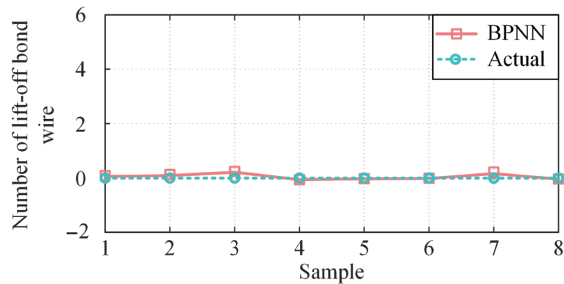

Fig. 22. Performance of the proposed AM method under case 2.

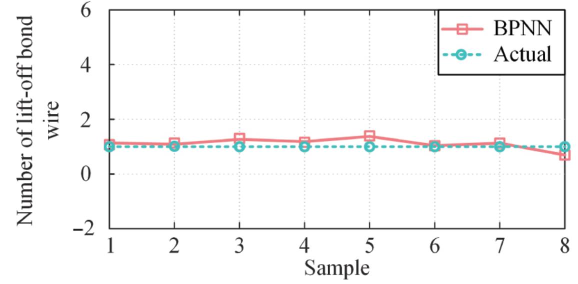

Fig. 23. Performance of the proposed AM method under case 3.

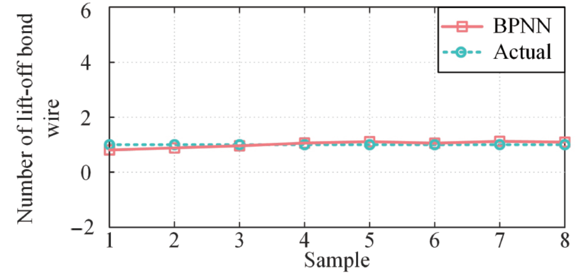

Fig. 24. Performance of the proposed AM method under case 4.

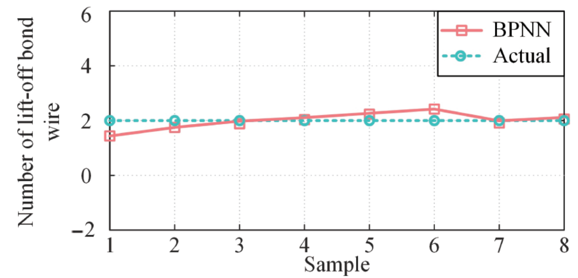

Fig. 25. Performance of the proposed AM method under case 5.

varied from 65.5 °C to 101.9 °C. With this, there are 320 data of the OVD that are used as the inputs of the BPNN, and the ratio of the training set to the test set is also given to 80%:20% during the training processes.

With the well-trained model, the bond wire monitoring performance of the proposed AM method is experimentally investigated, and the results are provided in Fig. 20. It is clear from Fig. 20 that the monitored lift-off bond wire provided by the proposed AM method makes a good agreement with the actual lift-off bond wire, thereby demonstrating the effectiveness of the proposed AM method. The monitoring errors of the proposed AM method lie in a limited range of ±0.4. According to the experimental results, it is known that the proposed AM method enables to provide accurate information of the BWD.

Figs. 21 and 22 show the performance of the proposed AM method with different junction temperature and different load currents. In the two cases, the number of the lift-off bond wire is set to 0 (that means the bond wire of the IGBT module is healthy), and the junction temperature is set to 88 °C and 95 °C, respectively. Based on the results in Figs. 23 and 24, the proposed AM method shows an acceptable performance in terms of bond wire AM. Additionally, it is worth noting that with different junction temperature of the IGBT module, an achievement of accurate AM is still made by using the proposed AM method.

Meanwhile, the performance of the proposed AM method with different junction temperature is further examined, and the results are presented in Figs. 23 and 24, in which 1 bond wire is lifted off. Seen from Figs. 23 and 24, the monitored lift-off bond wire agrees with the actual lift-off bond wire well, and the issue of junction temperature swings makes a negligible effect on the performance of the proposed AM method.

Moreover, the case of 2 lift-off bond wires with different junction temperature is implemented, and the results are shown in Figs. 25 and 26. It is suggested that in this case, the bond wire AM performance of the proposed AM method is acceptable, and the monitoring errors are within a reasonable range.

To further evaluate the performance of the proposed AM method, cases of 3 and 4 lift-off bond wires are carried out, which are shown in Figs. 27 and 28. The results in Figs. 27 and 28 indicate that the proposed AM method has the ability of providing the accurate information of the BWD.

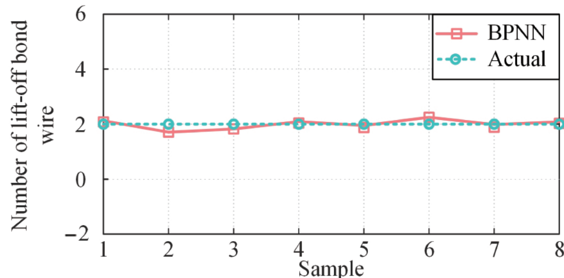

Fig. 26. Performance of the proposed AM method under case 6.

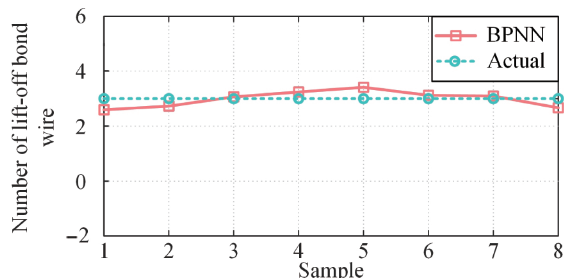

Fig. 27. Performance of the proposed AM method under case 7.

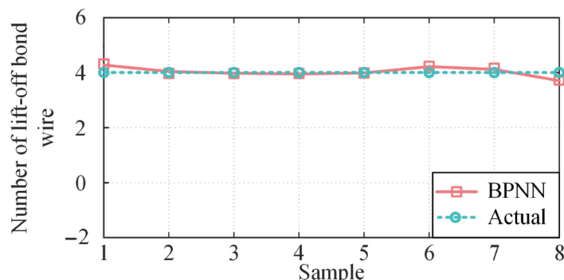

Fig. 28. Performance of the proposed AM method under case 8.

VI. Conclusion

This paper attempted a bond wire AM method based on the BPNN for IGBT modules. In the proposed AM method, the OVD is selected as the indicator of the BWD, and with the established multi-physical field coupling model of the IGBT module, the characterization behaviors of the OVD were thoroughly analyzed. The analyzed results revealed that the OVD shows a good sensitivity to the BWD but suffers from the serious performance degradation with junction temperature swings and load current dependence. Considering this, the BPNN is used in the proposed AM method to maintain the performance of bond wire AM under different operation conditions. Experimental tests were conducted to extensively investigate the performance of the proposed AM method. The results confirm that the proposed AM method exhibits a satisfactory performance of bond wire monitoring, and interesting benefits of avoiding the effects of junction temperature swings and load current dependence are achieved.

Nevertheless, the proposed AM method needs to cooperate with the junction temperature monitoring methods and measure the OVD of the IGBT modules, which may increase the complexity of the proposed AM method in practice. Notably, many studies have given feasible OVD measurement methods. In addition, the junction temperature extraction based on thermal network method can be used for the junction temperature information of the proposed method. Thus, further research efforts should be performed to achieve industrial applicability enhancement.

References

[1] J. Fang, F. Gao, and S. M. Goetz, “Symmetries in power electronics and lattice converters,” in *IEEE Transactions on Power Electronics*, vol. 38, no. 1, pp. 944–955, Jan. 2023.

[2] J. Fang, F. Blaabjerg, S. Liu, and S. M. Goetz, “A review of multilevel converters with parallel connectivity,” in *IEEE Transactions on Power Electronics*, vol. 36, no. 11, pp. 12468–12489, Nov. 2021.

[3] L. Li, P. Ning, X. Wen, and D. Zhang, “A 1200 V/200 a half-bridge power module based on Si IGBT/SiC MOSFET hybrid switch”, in *CPSS Transactions on Power Electronics and Applications*, vol. 3, no. 4, pp. 292–300, Dec. 2018.

[4] K. Chen, J. Dong, X. Ge, and Z. Xu, “A lifetime prediction method for IGBT modules considering the effects of multi-factors,” in *CPSS Transactions on Power Electronics and Applications*, vol. 8, no. 3, pp. 300–313, Sept. 2023.

[5] Y. Lu, E. Xiang, L. Zhu, H. Gao, H. Yang and R. Zhao, “Mission profile-based lifetime estimation and its system-controlled improvement method of IGBT modules for electric vehicle converters”, in *CPSS Transactions on Power Electronics and Applications,* vol. 8, no. 3, pp. 246–256, Sept. 2023.

[6] Y. Huang, Y. Luo, F. Xiao, B. Liu, and X. Tang, “Evaluation of the degradation in electrothermal characteristics of IGBTs during thermal cycling cocaused by solder cracking and Al-wires lifting-off based on iterative looping,” in *IEEE Transactions on Power Electronics*, vol. 38, no. 2, pp. 1768–1778, Feb. 2023.

[7] W. Liu, D. Zhou, F. Iannuzzo, M. Hartmann, and F. Blaabjerg, “Separation and validation of bond-wire and solder layer failure modes in IGBT modules,” in *IEEE Transactions on Industry Applications*, vol. 58, no. 2, pp. 2324–2331, Mar.-Apr. 2022.

[8] Y. Huang, Y. Jia, Y. Luo, F. Xiao, and B. Liu, “Lifting-off of Al bonding wires in IGBT modules under power cycling: Failure mechanism and lifetime model,” in *IEEE Journal of Emerging and Selected Topics in Power Electronics*, vol. 8, no. 3, pp. 3162–3173, Sept. 2020.

[9] K. Li, G. Y. Tian, L. Cheng, A. Yin, W. Cao, and S. Crichton, “State detection of bond wires in IGBT modules using eddy current pulsed thermography,” in *IEEE Transactions on Power Electronics*, vol. 29, no. 9, pp. 5000–5009, Sept. 2014.

[10] V. Smet, F. Forest, J. J. Huselstein, F. Richardeau, Z. Khatir, S. Lefebvre, and M. Berkani, “Ageing and failure modes of IGBT modules in high-temperature power cycling,” in *IEEE Transactions on Industrial Electronics*, vol. 58, no. 10, pp. 4931–4941, Oct. 2011.

[11] P. Godignon, X. Jorda, M. Vellvehi, X. Perpina, V. Banu, D. Lopez, J. Barbero, P. Brosselard, and S. Massetti, “SiC Schottky diodes for harsh environment space applications,” in *IEEE Transactions on Industrial Electronics*, vol. 58, no. 7, pp. 2582–2590, Jul. 2011.

[12] B. Ji, V. Pickert, W. Cao, and B. Zahawi, “In situ diagnostics and prognostics of wire bonding faults in IGBT modules for electric vehicle drives,” in *IEEE Transactions on Power Electronics*, vol. 28, no. 12, pp. 5568–5577, Dec. 2013.

[13] A. Singh, A. Anurag, and S. Anand, “Evaluation of Vce at inflection point for monitoring bond wire degradation in discrete packaged IGBTs,” in *IEEE Transactions on Power Electronics*, vol. 32, no. 4, pp. 2481–2484, Apr. 2017.

[14] P. Sun, C. Gong, X. Du, Y. Peng, B. Wang, and L. Zhou, “Condition monitoring IGBT module bond wires fatigue using short-circuit current identification,” in *IEEE Transactions on Power Electronics*, vol. 32, no. 5, pp. 3777–3786, May 2017.

[15] K. Wang, L. Zhou, P. Sun, and X. Du, “Monitoring bond wire defects of IGBT module using module transconductance,” in *IEEE Journal of Emerging and Selected Topics in Power Electronics*, vol. 9, no. 2, pp.

2201–2211, Apr. 2021.

[16] M. A. Eleffendi and C. M. Johnson, "In-service diagnostics for wire-bond lift-off and solder fatigue of power semiconductor packages," in *IEEE Transactions on Power Electronics*, vol. 32, no. 9, pp. 7187–7198, Sep. 2017.

[17] K. Hu, Z. Liu, H. Du, L. Ceccarelli, F. Iannuzzo, F. Blaabjerg, and I. A. Tasiu, "Cost-effective prognostics of IGBT bond wires with consideration of temperature swing," in *IEEE Transactions on Power Electronics*, vol. 35, no. 7, pp. 6773–6784, Jul. 2020.

[18] X. Wang, P. Sun, L. Sun, Q. Luo, and X. Du, "Online condition monitoring for bond wire degradation of IGBT modules in three-level neutral-point-clamped converters," in *IEEE Transactions on Industrial Electronics*, vol. 68, no. 8, pp. 7474–7484, Aug. 2021.

[19] Y. Yang and P. Zhang, "In situ junction temperature monitoring and bond wire detecting method based on IGBT and FWD on-state voltage drops," in *IEEE Transactions on Industry Applications*, vol. 58, no. 1, pp. 576–587, Jan.-Feb. 2022.

[20] J. Liu, G. Zhang, Q. Chen, L. Qi, Y. Geng, and J. Wang, "In situ condition monitoring of IGBTs based on the Miller plateau duration," in *IEEE Transactions on Power Electronics*, vol. 34, no. 1, pp. 769–782, Jan. 2019.

[21] A. Moazami, S. Mohsenzade, and K. Akbari, "An online condition monitoring method for IGBT gate oxide degradation based on the gate current in Miller plateau," in *IEEE Transactions on Industrial Electronics*, vol. 70, no. 9, pp. 9505–9514, Sep. 2023.

[22] Y. Yang and P. Zhang, "A novel bond wire fault detection method for IGBT modules based on turn-on gate voltage overshoot," in *IEEE Transactions on Industrial Electronics*, vol. 36, no. 7, pp. 7501–7512, Jul. 2021.

[23] W. Zhang, K. Tan, B. Ji, L. Qi, X. Cui, J. Wei, and X. Zhang, "In situ diagnosis of wire bonding faults for multichip IGBT modules based on the crosstalk effect," in *IEEE Journal of Emerging and Selected Topics in Power Electronics*, vol. 10, no. 5, pp. 5107–5117, Oct. 2022.

[24] K. Wang, L. Zhou, P. Sun, and X. Du, "Monitoring bond wires fatigue of multichip IGBT module using time duration of the gate charge," in *IEEE Transactions on Power Electronics*, vol. 36, no. 1, pp. 888–897, Jan. 2021.

[25] K. Wang, P. Sun, B. Zhu, Q. Luo, and X. Du, "Monitoring chip branch failure in multichip IGBT modules based on gate charge," in *IEEE Transactions on Industrial Electronics*, vol. 70, no. 5, pp. 5214–5223, May 2023.

[26] W. Zhang, K. Tan, B. Ji, L. Qi, X. Cui, X. Zhang, and L. Du, "In situ diagnosis of multichip IGBT module wire bonding faults based on collector voltage undershoot," in *IEEE Transactions on Industrial Electronics*, vol. 70, no. 3, pp. 3045–3054, Mar. 2023.

[27] J. Wang, W. Chen, Y. Wu, Y. Liu, T. Wang, L. Wang, J. Zhang, J. Liu, and Y. Gan, "In situ diagnosis for IGBT chip failure in multichip IGBT modules based on a newly defined characteristic parameter low-sensitive to operation conditions," in *IEEE Transactions on Power Electronics*, vol. 38, no. 6, pp. 7711–7722, Jun. 2023.

[28] S. Zhao, F. Blaabjerg, and H. Wang, "An overview of artificial intelligence applications for power electronics," in *IEEE Transactions on Power Electronics*, vol. 36, no. 4, pp. 4633–4658, Apr. 2021.

[29] Y. Zhang, Z. Wang, H. Wang, and F. Blaabjerg, "Artificial intelligence-aided thermal model considering cross-coupling effects," in *IEEE Transactions on Power Electronics*, vol. 35, no. 10, pp. 9998–10002, Oct. 2020.

[30] H. Wang, Z. Xu, X. Ge, Y. Liao, Y. Yang, Y. Zhang, B. Yao, and Y. Chai, "A junction temperature monitoring method for IGBT modules based on turn-off voltage with convolutional neural networks," in *IEEE Transactions on Power Electronics*, vol. 38, no. 8, pp. 10313–10328, Aug. 2023.

[31] Y. Peng and H. Wang, "Application of digital twin concept in condition monitoring for DC-DC converter," in *2019 IEEE Energy Conversion Congress and Exposition (ECCE)*, Baltimore, MD, USA, 2019, pp. 2199–2204.

[32] Y. Peng, S. Zhao, and H. Wang, "A digital twin based estimation method for health indicators of DC-DC converters," in *IEEE Transactions on Power Electronics*, vol. 36, no. 2, pp. 2105–2118, Feb. 2021.

[33] S. Zhao, S. Chen, F. Yang, E. Ugur, B. Akin, and H. Wang, "A composite failure precursor for condition monitoring and remaining useful life prediction of discrete power devices," in *IEEE Transactions on Industrial Informatics*, vol. 17, no. 1, pp. 688–698, Jan. 2021.

[34] S. Zhao, Y. Peng, Y. Zhang, and H. Wang, "Parameter estimation of power electronic converters with physics-informed machine learning," in *IEEE Transactions on Power Electronics*, vol. 37, no. 10, pp. 11567–11578, Oct. 2022.

[35] M. K. Kim, Y. D. Yoon, and S. W. Yoon, "Actual maximum junction temperature estimation process of multichip SiC MOSFET power modules with new calibration method and deep learning," in *IEEE Journal of Emerging and Selected Topics in Power Electronics*, vol. 11, no. 6, pp. 5602–5612, Dec. 2023.

[36] W M Haynes, *CRC Handbook of Chemistry and Physics*, 97th ed, CRC Press, 2016.

[37] M. Jiang, G. Fua, M. B. Fogsgaardb, A. S. Bahmanb, Y. Yang, and F. Iannuzzob, "Wear-out evolution analysis of multiple-bond-wires power modules based on thermo-electro-mechanical FEM simulation," in *Microelectronics Reliability*, vol. 100-101, pp. 113472–113477, Sep. 2019.

[38] J. Chen, E. Deng, P. Liu, S. Yang, and Y. Huang, "The Influence and Application of Bond Wires Failure on Electrothermal Characteristics of IGBT Module," in *IEEE Transactions on Components, Packaging and Manufacturing Technology*, vol. 11, no. 9, pp. 1426–1434, Sep. 2021.

[39] X. D. Li, G. Q. Lu, and Y. H. Mei, "Reliable aluminum wire-bonded SiC/Si diodes with laminated Al/Cu stress buffers," in *IEEE Transactions on Power Electronics*, vol. 37, no. 9, pp. 10149–10153, Sep. 2022.

[40] Y. Yang, Q. Zhang, and P. Zhang, "A novel on-line IGBT junction temperature measurement method based on on-state voltage drop," in *2019 22nd International Conference on Electrical Machines and Systems (ICEMS)*, Harbin, China, 2019, pp. 1–6.

[41] X. Perpiñà, J. F. Serviere, J. Saiz, D. Barlini, M. Mermet-Guyennet, and J. Millán, "Temperature measurement on series resistance and devices in power packs based on on-state voltage drop monitoring at high current," in *Microelectronics Reliability*, vol. 46, no. 9, pp. 1834–1839, Sep. 2016.

[42] Y. Li, W. Dong, Q. Yang, J. Zhao, L. Liu, and S. Feng, "An automatic impedance matching method based on the feedforward-backpropagation neural network for a WPT system," in *IEEE Transactions on Industrial Electronics*, vol. 66, no. 5, pp. 3963–3972, May 2019.

Gengle Liang received the B.S. degree in electrical engineering from the Southwest Jiaotong University, Chengdu, China, in 2022. He is currently pursuing the M.S. degree in electrical engineering at Southwest Jiaotong University. His research interests are the reliability of power semiconductor devices, such as SiC MOSFETs junction temperature monitoring and powerloss calculation.

Xinglai Ge received the B.S., M.S., and Ph.D. degrees in electrical engineering from Southwest Jiaotong University, Chengdu, China, in 2001, 2004, and 2010, respectively. He is currently a Full Professor in the School of Electrical Engineering, Southwest Jiaotong University and a Vice Director of Department of Power Electronics and Power Drive. From October 2013 to October 2014, he was a visiting scholar at the School of Electrical and Computer Engineering, Georgia Institute of Technology, Atlanta, GA, USA. He is the author and co-author of more than 70 technical papers. His research interests include stability analysis and control of electrical traction system, fault diagnosis and reliability evaluation of traction converter and motor drive system.

Huimin Wang received the B.Eng. and Ph.D. degrees in electrical engineering from Southwest Jiaotong University (SWJTU), Chengdu, China, in 2016 and 2021, respectively. From October 2019 to October 2020, he has been a Visiting Ph.D. Student with the Department of Energy Technology, Aalborg University, Aalborg, Denmark. He is currently a researcher with TongJi University. His research interests include AC motor drive system and its speed-sensorless control, synchronization techniques in grid-connected system, and reliability evaluation in traction drives. Dr. Wang was the recipient of one ESI Highly Cited Paper on *IEEE Journal of Emerging and Selected Topics in Power Electronics*, and the Best Paper Award of IEEE Transportation Electrification Conference and EXPO Asia-Pacific (ITEC Asia Pacific) in 2019.

Zhiliang Xu was born in Jiangxi Province, in 1999. He received the B.S. degree in electrical engineering from the Southwest Jiaotong University, Chengdu, China, in 2021. He is currently pursuing the M.S. degree in electrical engineering at Southwest Jiaotong University. His research interests are the reliability of power semiconductor devices, such as IGBT junction temperature monitoring.

Luo Dong was born in Jiangxi Province, in 1998. He received the M.S. degree in electrical engineering from the Southwest Jiaotong University, Chengdu, China, in 2023. His research interests are the reliability of power semiconductor devices, such as IGBTs electrical-thermal-mechanical coupling analysis and condition monitoring.

Yi Wang received the B.Eng. and M.S. degrees in electrical engineering from Southwest Jiaotong University, Chengdu, China, in 2002 and 2005, respectively. She is currently a deputy party secretary in the School of Electrical Engineering, Southwest Jiaotong University. Her research interests include control of electrical traction system, and reliability evaluation of traction converter and motor drive system.